Kinetic theory of positron-impact ionization in gases

G. J. Boyle,[1,*] W. J. Tattersall,[1,2] D. G. Cocks,[1] S. Dujko,[3] and R. D. White[1]
[1]*College of Science, Technology & Engineering, James Cook University, Townsville 4810, Australia*
[2]*Research School of Physics and Engineering, The Australian National University, Canberra, Australian Capital Territory 0200, Australia*
[3]*Institute of Physics, University of Belgrade, Pregrevica 118, 11080 Belgrade, Serbia*

(Received 19 March 2015; published 27 May 2015)

A kinetic theory model is developed for positron-impact ionization (PII) with neutral rarefied gases. Particular attention is given to the sharing of available energy between the postionization constituents. A simple model for the energy-partition function that qualitatively captures the physics of high-energy and near-threshold ionization is developed for PII, with free parameters that can be used to fit the model to experimental data. By applying the model to the measurements of Kover and Laricchia [Phys. Rev. Lett. **80**, 5309 (1998)] for positrons in H_2, the role of energy partitioning in PII for positron thermalization is studied. Although the overall thermalization time is found to be relatively insensitive to the energy partitioning, the mean energy profiles at certain times can differ by more than an order of magnitude for the various treatments of energy partitioning. This can significantly impact the number and energy distribution of secondary electrons.

DOI: 10.1103/PhysRevA.91.052710 PACS number(s): 34.80.Gs, 05.20.Dd, 51.10.+y, 34.80.Uv

I. INTRODUCTION

An understanding of the behavior of positrons in gases underpins many areas of technology and scientific research [1–5]. Of particular interest are applications to the medical imaging technique of positron emission tomography (PET) [6]. To optimize PET technologies and quantify the associated radiation damage requires a thorough understanding of the processes by which an energetic positron (and the secondary species) thermalize. It has been shown recently by Sanche [7–10] that the secondary electrons created via ionization can cause significant DNA damage. The number of secondary electrons ejected along the positron track is on the order of 10^4 per MeV of primary radiation produced in water [11,12], so it is clear that particular attention needs to be paid to the ionization process.

Although there has been extensive research on electrons in gases, positrons remain significantly less well understood. Specific collisional processes are available to the positron that do not exist for electrons, e.g., annihilation with an electron and positronium formation [13,14]. Although the impact from either a sufficiently energetic positron or electron can ionize a gas molecule, the ionization process differs in a crucial way: Ionization by positron impact is a particle-conserving process with respect to positrons, while ionization by electron impact is non-particle-conserving with respect to electrons [15–19]. The two types of ionization will be referred to as positron-impact ionization (PII) and electron-impact ionization (EII), respectively. In the framework of kinetic theory, Ness [20] developed a collision operator for EII, but no positron equivalent has yet been developed. Instead, previous investigations [21–26] have generally treated positron ionization as a simple excitation process that effectively assumes that the scattered positron receives all of the available postionization energy, although [27] has highlighted the effects of the secondary electron energy distribution.

In this paper, a PII equivalent of the EII collision operator of Ness is derived. Macroscopic transport coefficients, such as mean energy and flux drift velocity, are compared for a simple benchmark model using both a kinetic theory approach based on the Boltzmann equation and Monte Carlo simulation. Particular attention is paid to the effect of energy sharing between postionization constituents and the influence that different energy-partitioning models have on transport. A basic energy-partitioning model that captures, at least qualitatively, the physics of high-energy and near-threshold positron ionization is proposed, which can then be fitted to the rather limited experimental data that are available. The present kinetic theory model is used to investigate the transport of positrons in dilute H_2 gas using a recently compiled complete set of cross sections [4] and the proposed energy-partitioning model fitted to the experimental data of Kover and Laricchia [28].

II. THEORY

A. The kinetic equation and its multiterm solution

The fundamental equation describing a swarm of positrons moving through a dilute gaseous medium subject to an electric field $\mathbf{E}$ is the Boltzmann kinetic equation for the phase-space distribution function $f \equiv f(\mathbf{r},\mathbf{v},t)$ [24]:

$$\left(\frac{\partial}{\partial t} + \mathbf{v}\cdot\nabla + \frac{q\mathbf{E}}{m}\cdot\frac{\partial}{\partial \mathbf{v}}\right) f = -J(f), \tag{1}$$

where t is the time and $\mathbf{r}$, $\mathbf{v}$, q, and m are the position, velocity, charge, and mass of the positron, respectively. The right-hand side describes the effect of collisions on the distribution function at a fixed position and velocity. Essentially, the Boltzmann equation is an equation of continuity in phase space [29]. Solving Eq. (1) for the distribution function yields all relevant information about the system. Macroscopic transport properties including mean energy and drift velocity can then be found via averages over the ensemble as detailed in Sec. II C. The purpose of this paper is to investigate the effect of ionization, so for simplicity we will consider only spatially homogeneous situations.

If there is a single preferred direction in the system, e.g., due to an electric field in plane parallel geometry, then the angular dependence of the velocity component can be adequately described by an expansion in terms of Legendre polynomials

*Corresponding author: gregory.boyle@my.jcu.edu.au

[30], i.e., if $f(\mathbf{v},t) \rightarrow f(v,\mu,t)$, where $\mu = \hat{\mathbf{v}} \cdot \hat{\mathbf{E}}$, then

$$f(\mathbf{v},t) = \sum_{l=0}^{\infty} f_l(v,t) P_l(\mu), \tag{2}$$

where P_l is the lth Legendre polynomial [31]. Substituting the expansion (2) into Eq. (1) and equating the coefficients of Legendre polynomials results in the following coupled partial differential equations for the f_l in energy space:

$$\frac{\partial f_l}{\partial t} + \sum_{p=\pm1} \Delta_l^{(p)} \frac{qE}{m} \left(U^{1/2} \frac{\partial}{\partial U} + p \frac{l+(3p+1)/2}{2} U^{-1/2} \right) f_{l+p}$$
$$= -J_l(f_l) \quad (l = 0,1,2,\ldots,\infty), \tag{3}$$

where $U = \frac{1}{2} m v^2$, J_l is the Legendre decomposition of the collision operator, and

$$\Delta_l^{(+1)} = \frac{l+1}{2l+3},$$
$$\Delta_l^{(-1)} = \frac{l}{2l-1}.$$

Equation (3) represents an infinite set of coupled partial differential equations for the expansion coefficients f_l. In practice, one must truncate the series (2) at a sufficiently high index $l = l_{\max}$. The history of charged-particle transport in gases has been dominated by the two-term approximation [32], i.e., where only the first two terms have been included. The assumption of quasi-isotropy necessary for the two-term approximation is violated in many situations, particularly when inelastic collisions are included [33] or when higher-order moments are probed [34]. Such an assumption is not necessary in our formalism. Rather, $l_{\max}$ is treated as a free parameter to be increased until some convergence or accuracy criterion is met.

B. Collision operators in the multiterm representation

To solve Eq. (3) we require the collision operators for all of the relevant collisional processes and their representations in terms of Legendre polynomials J_l. If we assume that the neutral background gas is at rest and in thermal equilibrium at a temperature T_0, then the background medium has a Maxwellian distribution in velocity space and the collision operator is linear in the swarm approximation [35]. Below we detail the specific kinetic theory forms of the collision operator for conservative elastic and inelastic collisions, particle-loss collisions such as annihilation and positronium formation, and ionization, which is the focus of this work. A further expansion of each collision integral with respect to the ratio of swarm particle mass to neutral particle mass m/m_0 has been performed. Because this ratio is small for positrons (and electrons), only the leading term of this expansion for each collision process and in each equation of the system (3) was taken into account.

The total collision operator can then be separated for each of the different types of processes, e.g.,

$$J = J^{\text{el}} + J^{\text{in}} + J^{\text{ann}} + J^{\text{Ps}} + J^{\text{ion}},$$

where the right-hand-side terms represent the elastic, inelastic, annihilation, positronium formation, and ionization collision operators respectively. Microscopic scattering information is included via the appropriate scattering cross sections [14,36]. It is more natural to work with the collision frequency rather than the scattering cross sections directly. A collision frequency ν is defined for a particular process by

$$\nu(U) \equiv n_0 \sqrt{\frac{2}{m}} U^{1/2} \sigma(U), \tag{4}$$

where σ is the corresponding cross section of the process.

1. Conservative elastic and inelastic collisions

For particle-conserving elastic and inelastic collisions we assume the Wang-Chang *et al.* [37] semiclassical collision operator and its limiting cases. For an elastic collision, if all terms proportional to the mass ratio are neglected there is no energy transfer during a collision. To obtain a nonzero expression, a first-order mass ratio approximation is required [38], i.e.,

$$J_l^{\text{el}}(f_l) = \begin{cases} -\frac{2m}{m_0} U^{-1/2} \frac{\partial}{\partial U} \left[U^{3/2} \nu_1^{\text{el}}(U) \left(f_0 + kT_0 \frac{\partial f_0}{\partial U} \right) \right], & l = 0 \\ \nu_l^{\text{el}}(U) f_l, & l \geqslant 1, \end{cases}$$

where $\nu_l^{\text{el}} = n_0 \sqrt{2/m} U^{1/2} (\sigma_0^{\text{el}} - \sigma_l^{\text{el}})$ and σ_l is defined from the differential scattering cross section [36] $\sigma(U,\mu)$ via

$$\sigma_l(U) = 2\pi \int_0^{\pi} d\mu\, P_l(\mu) \sigma(U,\mu).$$

If the background gas has internal degrees of freedom then, to zeroth order in the mass ratio, energy exchange can still occur through excitation and deexcitation of those internal states. Hence, unlike the isotropic part of the elastic collision integral, the scalar part of the inelastic collision integral does not vanish under a zeroth-order mass assumption. The Legendre decomposed form of the inelastic collision operator in the cold gas limit is given by [39,40]

$$J_l^{\text{in}}(f_l) = \sum_j \nu_j^{\text{in}}(U) f_l$$
$$- \begin{cases} \left(\frac{U+U_j}{U} \right)^{1/2} \nu_j^{\text{in}}(U+U_j) f_l(U+U_j), & l = 0 \\ 0, & l \geqslant 1, \end{cases} \tag{5}$$

where the subscript j denotes the available inelastic channels, such as excitations and rotations, with an associated inelastic scattering cross section $\sigma_j^{\text{in}}(U)$ and a threshold energy U_j. It is implicit in the above equation that there is no thermal excitation of internal states.

2. Annihilation and positronium formation

Positron annihilation and positronium formation occur through distinctly different physical mechanisms. However, from a transport theory perspective they each represent a unidirectional particle loss process and hence the form of their collision operators are identical. Since there is no postcollision scattering the collision operator is simply [41]

$$J_l^{\text{loss}}(f_l) = \sum_k \nu_k^{\text{loss}}(U) f_l,$$

where k are the available loss process channels and ν_k^{loss} is the collision frequency for the kth loss process corresponding to the cross section $\sigma_k^{\text{loss}}(U)$.

3. Ionization

Ionization by electron impact is fundamentally different from ionization by positron impact. Since the ejected electron is of the same species as the impacting particle, EII is a non-particle-conserving process, i.e., the indistinguishability of electrons leads to a gain in the number of electrons in the swarm. Since the scattered positron can be distinguished from the ejected electron, PII is a particle-conserving process. A different collision operator needs to be used for each case. In previous studies, PII was treated as a simple excitation process, which ignores the possible partitioning of energy between the scattered positron and ejected electron. In what follows, we develop an explicit expression for the PII operator.

Following the approach of [20], the details of which are given in Appendix A, the PII collision operator takes the form

$$J_l^{\text{ion}}(f_l) = \nu^{\text{ion}}(U)f_l(U) - \begin{cases} \int \left(\frac{U'}{U}\right)^{1/2} P(U,U')\nu^{\text{ion}}(U')f_0(U')dU', & l=0 \\ 0, & l \geqslant 1, \end{cases} \tag{6}$$

where U' is the impact particle energy and ν^{ion} is the collision frequency for ionization, corresponding to an ionization cross section. The $P(U,U')$ term is the energy-partitioning function, defined such that $P(U,U')dU$ represents the probability of the positron having an energy in the range $U + dU$ for an incident positron of energy U'. The energy-partitioning function has the following properties:

$$P(U,U') = 0 \quad \text{for} \quad U' < U + U_I,$$

$$\int_0^{U'-U_I} P(U,U')dU = 1 \quad \text{for} \quad U' \geqslant U + U_I,$$

where U_I is the ionization threshold energy, i.e., the energy needed to overcome the electron binding. The energy sharing, which is determined by the energy-partitioning function P, is a major theme in the present work. It will be shown in Sec. V that different energy-partition models significantly affect positron transport.

C. Transport properties

The cross sections and collision operator terms represent the microscopic picture of positron interactions with the medium. The macroscopic picture, e.g., transport properties that represent experimental measurables, are obtained as averages of certain quantities with respect to the distribution function f. Among the transport properties of interest in the current paper are the number density n, flux drift velocity W, and mean energy ε of the positron swarm, which can be calculated via [35]

$$n = 2\pi\left(\frac{2}{m}\right)^{3/2}\int dU\, U^{1/2} f_0(U),$$

$$W = \frac{1}{n}\frac{2\pi}{3}\left(\frac{2}{m}\right)^{2}\int dU\, U f_1(U),$$

$$\varepsilon = \frac{1}{n}2\pi\left(\frac{2}{m}\right)^{3/2}\int dU\, U^{3/2} f_0(U).$$

The focus of this paper is the ionization process, so it is also useful to calculate the average ionization collision rate defined by

$$\alpha^{\text{ion}} = \frac{1}{n}2\pi\left(\frac{2}{m}\right)^{2}\int dU\, U^{1/2}\nu^{\text{ion}}(U) f_0(U).$$

III. NUMERICAL APPROACH FOR A MULTITERM SOLUTION

In this section we detail a numerical solution of the system of coupled ordinary differential equations (3) once an l-index truncation has been applied.

A. Method of lines

The method of lines (MOL) [42,43] is a technique for solving partial differential equations (PDEs) in which all but one dimension is discretized. In developing a numerical solution to the Boltzmann equation, we choose to first discretize the energy (or, equivalently, speed) space. In general, applying the MOL to linear PDEs results in a system of equations of the form

$$\mathbf{M}\frac{d}{dt}\mathbf{u} = \mathbf{L}\mathbf{u}, \tag{7}$$

where $[u]_i = u_i(t) \equiv u(x_i,t)$ and $\mathbf{L}$ and $\mathbf{M}$ are matrices resulting from the discretization process, commonly known as the stiffness matrix and mass matrix, respectively [44]. The formerly continuous variable x has been discretized into a set of x_i for $i = 0,1,\ldots,n$. The MOL formalism allows easy implementation of linear boundary conditions or constraints via the mass matrix. Let the discretized boundary conditions and constraints of (7) be represented by $\mathbf{G}\mathbf{u} = \mathbf{0}$, where $\mathbf{G}$ is a matrix and $\mathbf{0}$ represents a vector of zeros. Then clearly $\frac{d}{dt}\mathbf{G}\mathbf{u} = \mathbf{G}\frac{d}{dt}\mathbf{u} = \mathbf{0}$ and, provided the initial solution satisfies the constraints

$$\overline{\mathbf{M}}\frac{d}{dt}\mathbf{u} = \overline{\mathbf{L}}\mathbf{u}, \tag{8}$$

where $\overline{\mathbf{M}}$ and $\overline{\mathbf{L}}$ are the modified mass and stiffness matrices,

$$\overline{\mathbf{M}} = \begin{bmatrix}\mathbf{G}\\ \mathbf{M}\end{bmatrix}, \quad \overline{\mathbf{L}} = \begin{bmatrix}\mathbf{0}\\ \mathbf{L}\end{bmatrix}.$$

In a pure MOL approach, the system of ordinary differential equations (ODEs) (8) is solved analytically. However, one is eventually forced to discretize the time variable as well for complicated systems of equations, such as those arising from the discretization of the Boltzmann equation. In this work we choose to discretize the time dimension with a first-order implicit Euler method [45], for its good stability properties. Applying the implicit Euler method to Eq. (7) or (8) gives

$$(\mathbf{M} - h\mathbf{L})\mathbf{u}^{n+1} = \mathbf{M}\mathbf{u}^n, \tag{9}$$

where $\mathbf{u}^n$ and $\mathbf{u}^{n+1}$ are the solution vector $\mathbf{u}$ at times t_n and t_{n+1} and $h = t_{n+1} - t_n$ is the time step. For linear systems, Eq. (9) can be solved directly with linear algebra techniques.

B. Finite-difference representation in energy space

The finite-difference method [46] is a local approximation method that seeks to replace the continuous derivatives by a weighted difference quotient of neighboring points. It is widely used, simple to program, and leads to sparse matrices with band structures approximating derivatives [47]. Similar to the work of Winkler and co-workers [15,48,49], the system of ODEs is discretized at centered points using a centered difference scheme, i.e.,

$$\left.\frac{df(U,t)}{dx}\right|_{U_{i+1/2}} = \frac{f(U_{i+1},t) - f(U_i,t)}{U_{i+1} - U_i},$$

$$f(U_{i+1/2},t) = \frac{f(U_{i+1}) + f(U_i)}{2}.$$

Although a general form can be constructed for an arbitrary grid, the simplest case is for evenly spaced points, i.e.,

$$U_i = i\Delta U, \quad 0 \leqslant i \leqslant n,$$

where ΔU is a constant. Discretizing at the center between two solution nodes results in a system of linear equations that is underdetermined. The extra information is naturally provided by boundary conditions that are appended to the system.

C. Initial and boundary conditions

In positron experiments [13], unmoderated positrons have a peak in their emission energy spectrum of around half an MeV, which then lose energy rapidly via collisions. There is little information about the initial source distribution in thermalization experiments [50]. For our purposes, we wish to probe the influence of PII collisions and accordingly choose an initial distribution with a mean energy far above the ionization threshold so that a large range of the ionization cross section can be sampled during relaxation. One of the source distributions used by Campeanu and Humberston [50] in their investigations of helium is a distribution that is constant in speed space up to some sufficiently high cutoff value $v_{\max} = \sqrt{2U_{\max}/m}$, i.e., $f_0(v) = \Theta(v_{\max} - v)C$, where $\Theta(x)$ is the Heaviside step function. The mean energy of this distribution function is given by $\varepsilon = \frac{3}{5}U_{\max}$. We use this type of initial distribution for our investigations of thermalization and choose $U_{\max}$ to be sufficiently high to sample the ionization cross sections accordingly.

The system of coupled equations (3) requires boundary conditions on the expansion coefficients f_l. Winkler and co-workers [15,48,49] have analyzed the multiterm even-order approximation and discovered that the general solution of the steady-state hierarchy contains $\frac{1}{2}(l_{\max}+1)$ nonsingular and $\frac{1}{2}(l_{\max}+1)$ singular fundamental solutions when U approaches infinity and the physically relevant solution has to be sought within the nonsingular part. They give the boundary conditions necessary for the determination of the nonsingular physically relevant solution as

$$f_l(U=0) = 0 \quad \text{for odd } l,$$

$$f_l(U=U_\infty) = 0 \quad \text{for even } l,$$

$$f_l(U>U_\infty) = 0 \quad \text{for all } l,$$

where U_∞ represents a sufficiently large energy. In practice, U_∞ has to be determined in a prior calculation and is chosen such that the value of $f_0(U_\infty)$ is less than 10^{-10} of the maximum value of f_0.

IV. MONTE CARLO SIMULATION

The Monte Carlo simulation code employed in the current investigation is a particle-tracking model, similar in most respects to those described in [51,52]. For brevity, we shall only describe the different features that are necessary to carry out the ionization simulations featured in this paper. For further details of the simulation procedure the reader is referred to [53].

The treatment of ionization by the Monte Carlo code depends on the type of transport particle. For positron-impact ionization, since we are not interested in the transport of the resulting electrons to determine positron properties, we treat ionization as an inelastic process where the amount of energy that is lost is sampled from the ionization energy partitioning function $P(U,U')$ using inverse transform sampling [54]. For the partitioning functions used here, the cumulative probability distribution can be calculated analytically, which simplifies this procedure significantly.

For electron-impact ionization, we must include the impact of the additional electrons in the statistical model of the swarm. However, if the ionization rates are high, tracking the subsequent motion of every generated particle becomes computationally infeasible. Instead, we employ a form of Russian roulette variance reduction [55], where in an ionization event we select only one of the two postcollision electrons to continue tracking. Each selection has an equal probability of choosing either the original or ejected electron, so the selected electrons form a representative sample of all electrons that otherwise would have been in the swarm. Each resulting electron must then contribute towards the statistical measures of the swarm with a weighting that is twice as much as the precollision electron. Note that this can happen many times for one electron track and after n ionization events, the resulting electron will have a statistical weight of 2^n.

Sampling the transport coefficients presented below is performed in a manner similar to that in [53], except for the inclusion of the statistical weighting factor for each particle. For example, the mean value of a particle property ϕ at a single time is given by

$$\langle\phi\rangle = \frac{\sum_{i=1}^{N} w_i\phi_i}{\sum_{i=1}^{N} w_i},$$

where N is the number of electrons and w_i and ϕ_i are the statistical weight and measured property of the ith electron, respectively. The flux and bulk drift velocities employ this type of weighted mean in the following expressions:

$$W_{\text{flux}} = \langle v_z\rangle,$$

$$W_{\text{bulk}} = \tfrac{d\langle r_z\rangle}{dt},$$

where v_z and r_z are, respectively, the velocity and position of the particle along the axis of the electric field. Note that for positron-impact ionization there is no difference between the two drift velocities, because the number of positrons in the system is a conservative quantity.

V. RESULTS AND DISCUSSION

In this section we apply both the kinetic theory and Monte Carlo techniques detailed in the previous sections to describe positron transport in a benchmark model and positron transport in real H_2 gas. Comparisons are made to EII where possible. Particular attention is given to the role of energy partitioning between the scattered and ejected particles postionization, and a simple energy-partitioning model is proposed to capture the underlying physics.

A. Positron ionization benchmarking

We first discuss several benchmark models for EII that can act as a test bed for our numerical techniques and solution model. The Lucas-Saelee [56] model is a popular benchmark, but focuses on the differences between excitation and ionization rather than energy partitioning specifically. Taniguchi *et al.* [57] modified the partition function of the Lucas-Saelee model, which assumes a distribution with all energy-sharing fractions equiprobable, to instead share energy equally between the two electrons, but found that it did not alter the transport coefficients significantly. Instead, Ness and Robson [41] proposed a step model for testing energy sharing for EII, which was shown to have some variation for the partitionings they investigated. The details of the model are

$$\begin{aligned} \sigma_0^{\mathrm{el}} - \sigma_l^{\mathrm{el}} &= 10\ \text{Å}^2, \\ \sigma^{\mathrm{in}} &= \begin{cases} 1\ \text{Å}^2, & U \geqslant 10\ \mathrm{eV} \\ 0, & U < 10\ \mathrm{eV}, \end{cases} \\ \sigma^{\mathrm{ion}} &= \begin{cases} 1\ \text{Å}^2, & U \geqslant 15\ \mathrm{eV} \\ 0, & U < 15\ \mathrm{eV}, \end{cases} \\ m_0 &= 25\ \mathrm{amu}, \\ T_0 &= 0\ \mathrm{K}. \end{aligned} \tag{10}$$

Transport coefficients for EII calculated using kinetic theory are compared against the results of Ness and Robson and the Monte Carlo simulations in Table IV of Appendix B. The results support the integrity of our methods and solutions. Transport coefficients for PII under this model are given in Table I for varying energy-sharing fractions Q, where $Q = \frac{U}{U'-U_I}$. As described in Appendix A, the collision operator (6) breaks down when $Q = 0$, hence there is no value given in Table I corresponding to the kinetic model for positrons with $Q = 0$. We are unaware of any previous positron-impact calculations for model (10), so the transport properties from our kinetic theory model are compared solely against an independent Monte Carlo simulation in Table I. The uncertainty in the Monte Carlo simulations has been estimated to be less than 1% for the ionization collision rates and less than 0.5% (generally less than 0.3%) for the drift velocity and mean energy. The two approaches give $\alpha^{\mathrm{ion}}/n_0$, ε, and W values that differ by less than 0.6%, 0.3%, and 0.3%, respectively, over the range of reduced electric fields and available energy fractions, all of which are within the corresponding Monte Carlo uncertainty. As the reduced field E/n_0 is increased, the velocity distribution function samples more of the ionization process leading to a greater ionization rate and a stronger dependence of the transport coefficients on the postcollision energy partitioning.

The convergence of transport coefficients for 1000 Td with increasing l_{max} is shown in Table II. Since an even-order approximation is required for the appropriate boundary conditions, the l_{max} are odd in our calculations. Clearly the two-term approximation ($l_{\mathrm{max}} = 1$) leads to an overestimation of the ionization rate, mean energy, and flux drift velocity by approximately 2%. Indeed, six terms are required to achieve convergence to four significant figures.

The variation of mean energy with Q for PII at a reduced electric field of 800 Td is shown in Fig. 1. For PII, the mean energy of the positron swarm increases monotonically with the energy-sharing fraction Q. This behavior is to be expected, as the ejected electron directly removes energy from the positron swarm. The ionization collision frequency increases with energy in model (10), so the greater the energy of the

TABLE I. Comparison of average ionization rates $\alpha^{\mathrm{ion}}/n_0$, mean energies ε, and flux drift velocities W for PII for model (10) for different reduced fields E/n_0 and energy-sharing fractions Q. Columns labeled "Current" correspond to the current kinetic theory calculations and columns labeled "MC" are the results of the Monte Carlo simulation. Note that a Q entry of AFE corresponds to all fractions equiprobable.

E/n_0		$\alpha^{\mathrm{ion}}/n_0$ (10^{-15} m^3 s^{-1})		ε (eV)		W (10^5 ms^{-1})	
(Td)	Q	Current	MC	Current	MC	Current	MC
300	0		1.711		6.869		2.767
	1/4	1.720	1.718	6.919	6.931	2.722	2.730
	1/3	1.725	1.719	6.940	6.942	2.711	2.706
	1/2	1.740	1.739	6.983	6.979	2.693	2.689
	2/3	1.757	1.761	7.021	7.023	2.677	2.676
	3/4	1.767	1.774	7.041	7.040	2.671	2.664
	1	1.807	1.804	7.098	7.087	2.654	2.648
	AFE	1.745	1.739	6.979	6.981	2.699	2.701
500	0		4.856		9.210		3.951
	1/4	4.915	4.917	9.379	9.375	3.819	3.822
	1/3	4.955	4.949	9.446	9.450	3.789	3.780
	1/2	5.060	5.055	9.579	9.588	3.738	3.739
	2/3	5.211	5.208	9.716	9.714	3.697	3.697
	3/4	5.288	5.293	9.788	9.789	3.678	3.678
	1	5.565	5.599	10.03	10.05	3.627	3.628
	AFE	5.119	5.107	9.589	9.577	3.754	3.755
800	0		9.903		13.30		5.260
	1/4	10.21	10.23	13.75	13.76	4.986	4.992
	1/3	10.39	10.40	13.93	13.93	4.922	4.925
	1/2	10.84	10.83	14.32	14.33	4.816	4.818
	2/3	11.40	11.41	14.79	14.81	4.719	4.725
	3/4	11.68	11.70	15.07	15.09	4.672	4.678
	1	12.92	12.95	16.27	16.31	4.518	4.527
	AFE	10.92	10.94	14.38	14.36	4.850	4.857

TABLE II. Convergence of transport properties with l_{max} for the PII model (10) at 1000 Td and $Q = 1/2$.

l_{max}	$\alpha^{\mathrm{ion}}/n_0$ (10^{-15} m^3 s^{-1})	ε (eV)	W (10^5 ms^{-1})
1	12.77	18.23	5.460
3	12.47	17.96	5.350
5	12.48	17.95	5.349
7	12.48	17.95	5.349

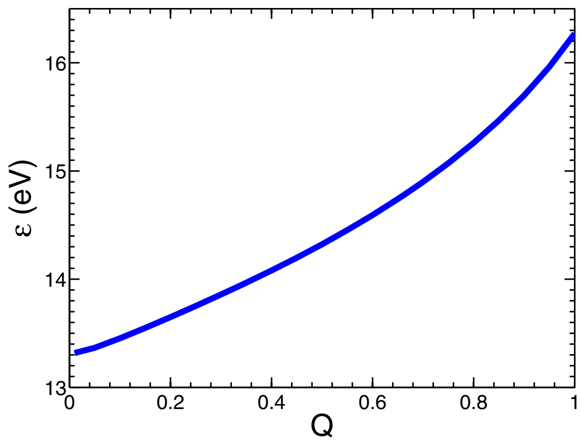

FIG. 1. (Color online) Variation of mean energy ε with the energy-sharing fraction Q for the PII model (10) at a reduced field of 800 Td.

swarm, the higher the rate of ionization collisions. Hence α^{ion}/n_0 also increases monotonically with Q. The flux drift velocity W, in contrast, decreases with increasing Q. The effect of collisions is to randomize the directions of the swarm particles such that an increase in the ionization rate decreases the average velocity of the swarm. The transport properties for the all fractions equiprobable (AFE) distribution are very similar to that of the equal-energy-sharing case.

The variation of mean energy with Q for EII at 800 Td is shown in Fig. 2. The mean energy profile is symmetrical about $Q = 0.5$ due to the indistinguishability of postcollision electrons and for 800 Td has a concave shape with a minimum value corresponding to equal energy sharing. It should be noted that, in contrast to PII where the mean energy always increases with Q, the exact nature of the EII mean energy profile depends on how the distribution function samples the elastic, inelastic, and ionization cross sections. The variation in the transport properties for EII with respect to Q for the fields considered is small, suggesting that EII is relatively insensitive to the exact nature of the energy partitioning for the model (10). Ness and Makabe [58] have shown that for EII in argon the choice of energy-sharing fraction can in fact cause differences

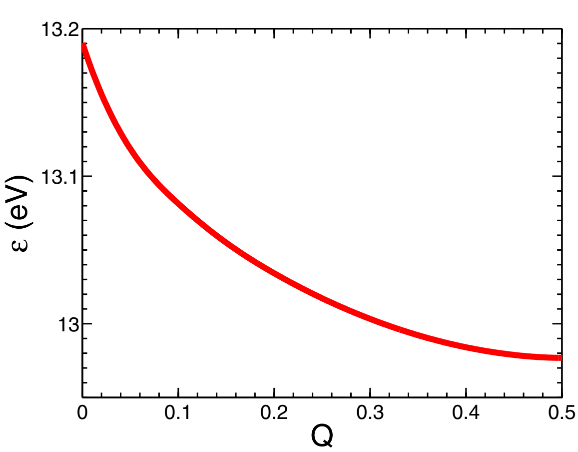

FIG. 2. (Color online) Variation of mean energy ε with the energy-sharing fraction Q for the EII model (10) at a reduced field of 800 Td.

of ~25%, so care must still be taken when choosing the energy-partitioning function.

The qualitative shape of the Q dependence of the mean energy for PII is insensitive to the reduced electric field and the range of values for a particular reduced field is considerably larger than that for EII. In previous positron studies [15,17,23,59], PII has been treated as a standard excitation process. The current results suggest that PII is particularly sensitive to the form of the energy partitioning and if real-world PII differs significantly from the model of pure scattering with excitation, large errors can result. To comment on this, we need to develop a realistic model of PII energy partitioning.

B. Positron ionization energy-partitioning model

We now wish to develop a model for postionization energy partitioning that captures the following basic physical behaviors.

(i) For high impact energies, the positron ionization scattering cross section approaches the electron ionization scattering cross section. The first Born approximation [60] is valid for high impact energies and shows a heavy bias towards the case where the scattered positron leaves the collision with almost all of the energy that is available postcollision.

(ii) For impact energies near the ionization threshold, there is significant correlation between the scattered positron and ejected electron. In the Wannier theory [61] originally developed for near-threshold EII, the repulsion between the two electrons cause them to emerge with similar energies but in opposite directions. In terms of the interaction potential between the two electrons, one may talk about a Wannier ridge upon which the system is in an unstable equilibrium. Klar [62] was the first to adapt Wannier's classical idea to PII. As in Wannier's theory, the energy is predicted to be shared equally, however now the positron and electron emerge in similar directions due to the Coulomb attraction. Ashley *et al.* [63] measured the positron ionization cross section in helium, which they were able to accurately represent by a power law, albeit different from that derived by Klar. Ihra *et al.* [64] extended the Wannier theory to be consistent with both Klar and experiment. The success of these power-law models justifies the assumption of equal energy sharing at near-threshold impact energies, although recent experiments [65] suggest a slight asymmetry. It should be noted that the positron and electron escape in similar directions with similar energies and are highly correlated, so no clear distinction between ionization and continuum state positronium can be made [13].

(iii) Ionization at intermediate energies appears to be a combination of the above two effects, i.e., a strong peak in the energy-sharing distribution corresponding to the scattered positron leaving with all the available energy and a second peak occurring when the positron and electron emerge with similar energy and direction and in a highly correlated state. This feature has been shown in the studies of atomic hydrogen by Brauner *et al.* [66] and measured experimentally in H_2 by Laricchia and co-workers [28,65].

To capture simply the above three characteristics we propose a model consisting of an exponentially decaying function

$g_{\mathrm{high}}(Q)$ to represent the high-impact-energy ionization and a rational polynomial (sometimes called the Cauchy or Lorentz distribution) $g_{\mathrm{low}}(Q)$ centered around equal energy sharing to represent the near-threshold ionization, i.e.,

$$g_{\mathrm{high}}(Q) = A_{\mathrm{high}} \exp(\beta_{\mathrm{high}} Q), \tag{11}$$

$$g_{\mathrm{low}}(Q) = A_{\mathrm{low}}\left[\beta_{\mathrm{low}}^2 + (Q-0.5)^2\right]^{-1}, \tag{12}$$

where Q is the fraction of the available energy, A_{high} and A_{low} are normalization constants, and β_{high} and β_{low} are free parameters to be fitted. An energy-fraction-partitioning function that depends only on the impact energy and Q can then be constructed as

$$g(U',Q) = w(U')g_{\mathrm{high}}(Q) + (1-w(U'))g_{\mathrm{low}}(Q), \tag{13}$$

where $w(U')$ is chosen as a hyperbolic tangent function to transition smoothly between g_{high} and g_{low}, i.e.,

$$w(U') = \frac{1}{2}\left[1 + \tanh\left(\gamma\frac{U'-U_I}{q} - \delta\right)\right], \tag{14}$$

where q is the elementary charge and γ and δ are free parameters that control where and how sharp the transition is. The relationship between the energy-fraction-partitioning function $g(U',Q)$ and the energy-partitioning function $P(U,U')$ used in Eqs. (6) and (A7) is given simply by

$$g(U',Q)Q = P(U,U')U.$$

In the following sections we investigate a test model with reasonable values for the free parameters that can serve as a future benchmark model and then fit the energy-partitioning model to real experimental H_2 data.

1. *Test model*

In this section we investigate the effect that the energy-partitioning model (11)–(14) has on positron transport for a range of reduced electric-field strengths. The parameters for the energy-partitioning function are

$$\beta_{\mathrm{high}} = 10, \quad \beta_{\mathrm{low}} = 0.05,$$
$$\gamma = 0.05, \quad \delta = 3.5, \tag{15}$$

with the same cross sections, neutral temperature, and mass as model (10). The energy-partition function for model (15) is displayed in Fig. 3.

Transport properties calculated via kinetic theory and Monte Carlo are shown in Table III. The kinetic theory and Monte Carlo results agree to within 0.4%. Also included in the table for 800 and 5000 Td are the swarm properties assuming the energy partitioning was replaced by only g_{low} or g_{high}, respectively. At 800 Td, the swarm properties for the full energy-partitioning model are close to that which results from the inclusion of only g_{low}, which indicates that the distribution is generally sampling the even-energy-sharing part of the full energy-partitioning distribution. At the higher field of 4000 Td the swarm properties are now close to those that come from allowing only g_{high} to have an effect. As the field has increased, the distribution has shifted from sampling mostly the even-sharing region to the region that is heavily biased towards the positron getting large amounts of available energy.

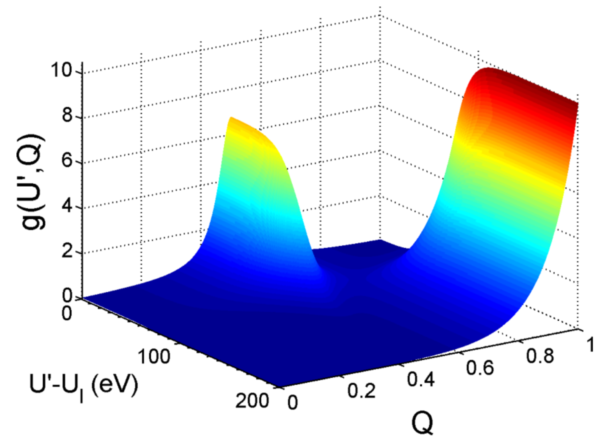

FIG. 3. (Color online) Variation of the energy-fraction-partition function with impact energy, relative to the ionization threshold, and energy-sharing fraction Q for the parameters in (15).

2. *Model for positron-impact ionization in* H_2

Laricchia and co-workers [28,65] have measured experimentally the energy sharing of postionization species for PII for a specific impact energy and angle. Their results for ionization by a 100-eV positron, where both the positron and electron emerge at the same angle of 0°, are included in Fig. 4. It is evident that there is a bias towards the positron getting all or large amounts of the available energy, with a secondary peak close to equal energy sharing due to electron-positron correlation effects. Our model predicts that this peak should occur at exactly $Q = 0.5$, but experiments show that there is a slight energy-sharing asymmetry in positron ionization such that the peak actually occurs at $Q > 0.5$ [65]. A more sophisticated energy-partitioning model will need to take this effect into account. We have performed a nonlinear least-squares calculation to fit the free parameters of model (11)–(14) to the experimental data, which were determined to

TABLE III. Comparison of average ionization rate $\alpha^{\mathrm{ion}}/n_0$, mean energies ε, and flux drift velocities W for PII for model (15). Columns labeled "Current" correspond to the current kinetic theory calculations and columns labeled "MC" are the results of Monte Carlo simulation.

E/n_0	$\alpha^{\mathrm{ion}}/n_0$ (10^{-15} m^3 s^{-1})		ε (eV)		W (10^5 ms^{-1})	
(Td)	Current	MC	Current	MC	Current	MC
800	10.92	10.90	14.40	14.37	4.810	4.814
800[a]	10.86	10.85	14.35	14.32	4.816	4.820
800[b]	12.48	12.37	15.82	15.70	4.555	4.585
1600	26.29	26.26	34.12	34.04	6.331	6.348
2400	40.97	40.88	65.56	65.42	6.910	6.932
3200	53.97	53.85	104.1	103.9	7.201	7.229
4000	64.95	64.90	144.8	145.0	7.491	7.517
4000[a]	49.18	49.11	86.49	86.52	9.509	9.527
4000[b]	66.96	66.64	149.5	149.2	7.150	7.178

[a] $w(U) = 0$.
[b] $w(U) = 1$.

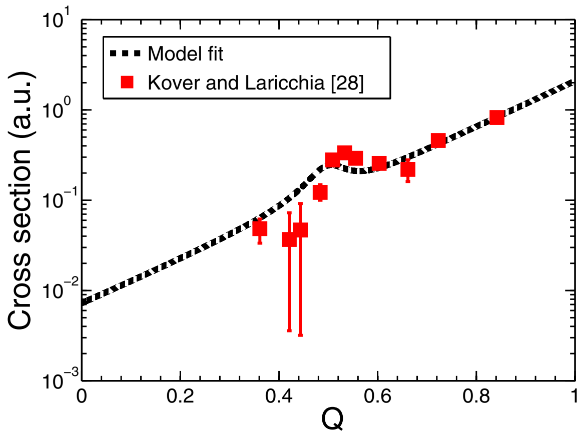

FIG. 4. (Color online) Differential PII cross section for an impact energy of 100 eV, as a function of the energy-sharing fraction Q. Large (red) squares are the experimental data of Kover and Laricchia [28] for the triply differential cross section for an impact energy of 100 eV and ejection angle of 0°. The model fit has been calculated with the parameters in (16) and by assuming that the triply differential cross section is the same at all ejection angles.

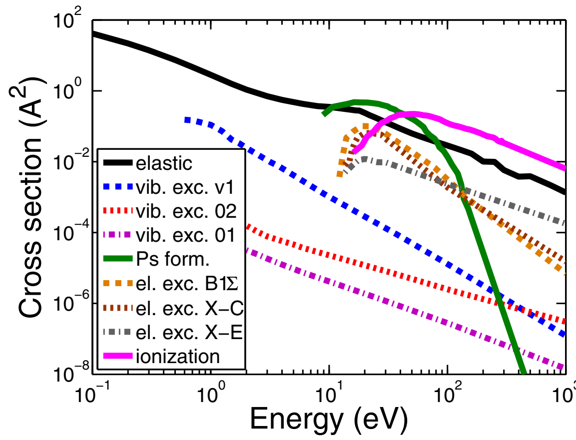

FIG. 5. (Color online) Cross section set for positron scattering in H_2. References are given in the text.

be

$$\beta_{\text{high}} = 5.88, \quad \beta_{\text{low}} = 0.0468,$$
$$\gamma = 0.0584, \quad \delta = 3.45. \qquad (16)$$

The fitted profile is shown in Fig. 4 and qualitatively reproduces the main features of the experiment. It should be noted that at the 0° scattering angle the secondary peak is particularly dominant and if one were to average the triple-differential cross section over all angles, a similar form with a reduced secondary peak would result. Due to the lack of experimental data at a variety of angles, we will assume that the angle-integrated cross section has the exact same shape as the 0° angle cross section for the purpose of this paper, which will have the effect of exaggerating the equal-energy-sharing part of the full energy-sharing distribution. The parameters in Eq. (16) have been chosen to ensure a smooth transition between g_{low} and g_{high} while ensuring that the relative weights give the fit to experiment for an impact energy of 100 eV. The full three-dimensional energy-sharing distribution is qualitatively similar to Fig. 3.

C. Positrons in molecular hydrogen

In the previous section, a model for the postionization energy sharing for PII from H_2 was proposed. In this section, the effect of the energy sharing on transport properties is investigated for PII in rarefied H_2. The set of H_2 cross sections employed is that compiled in [4,26] and using the elastic cross section of [67] calculated with a convergent-close-coupling formalism [68] up to 1000 eV, extrapolating where necessary (see Fig. 5). It is clear that the ionization process, which turns on at 15.4 eV is particularly important and dominates at energies above 50 eV.

In order to assess the importance of energy partitioning on ionization we investigate the time dependence of the mean energy for a source of positrons in H_2 gas at 293 K, as they relax to thermal equilibrium in the absence of an electric field. The source distribution is chosen to be uniform in velocity space up to the 1000-eV cutoff, which is equivalent to an initial mean energy of 600 eV. The thermalization profiles for the energy-partitioning model (16) and using the PII collision operator with $Q = 0.5$ (equal energy sharing) and $Q = 1$ (standard excitation form) are shown in Fig. 6. There are two distinct regions of rapid relaxation, one due to ionization at high energies and one due to the vibrational modes at lower energies. The first occurs on time scales of between 0.1 and 2 ns amagat and the second at about 5 ns amagat, which shows that the relaxation due to inelastic collisions is very rapid. While in the ionization-dominated region, the three profiles show significant differences in mean energy of up to an order of magnitude. The profile corresponding to $Q = 1.0$ has the highest mean energy since the positron loses the least amount of energy during an ionization collision

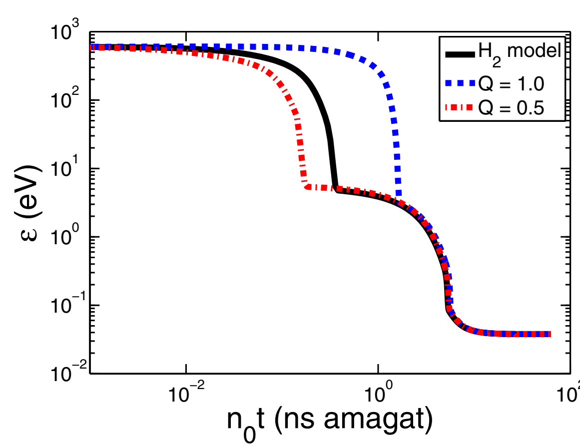

FIG. 6. (Color online) Mean energy temporal relaxation of a positron swarm in H_2 at 293 K. The initial source distribution is uniform in speed space up to 1000 eV. The H_2 model ionization parameters are given in Eq. (16) and are compared with constant energy-sharing fractions of $Q = 0.5$ and 1.0.

in that limit. It takes significantly longer to relax until the positron energies fall below the ionization region and thus they will experience more ionization collisions. The $Q = 0.5$ profile shows the lowest mean energy since the ejected electron removes large amounts of energy from the swarm and exits the ionization region quickest. The real H_2 model profile sits between the even-energy-sharing and standard excitation profiles as expected, since it is essentially a mixture of the two. At lower energies, once ionization collisions become insignificant, all three energy-partitioning profiles coalesce, resulting in essentially the same total thermalization times.

Although the total thermalization time is essentially insensitive to the form of the ionization energy partitioning, the large differences in mean energies in the ionization-dominated region can have other important effects. In a space-dependent situation, the higher mean energies can allow the positron to travel larger distances during thermalization. This is important to PET simulations since the resolution of PET images is dependent on the distances traveled between positron emission and annihilation [6]. Similarly, the higher the mean energy, the longer the positron swarm can significantly sample the ionization cross section and hence the more secondary electrons that are created via PII. It is the secondary electrons created in the human body during PET scans that can cause DNA damage [7–10]. Furthermore, the exact energy profile of the secondary electrons will be dependent on the form of the PII energy partitioning.

VI. CONCLUSION

Ionization by positron impact is a fundamentally different process than ionization by electron impact. Applications such as PET demand increasingly accurate models for positron transport, so it is important to be able to describe the ionization process in detail. To this end, a kinetic theory model with a general PII collision operator has been developed. The key feature of the ionization collision operator is the energy-partition function, which controls how the available energy is shared between the postcollision constituents.

The kinetic theory results were compared against a Monte Carlo simulation for a simple test model (10), which may serve as a benchmark for ionization. The transport properties calculated differed between the two approaches by less than 0.6% over a range of reduced electric fields and available energy fractions, which is within their respective uncertainties. The sensitivity of the transport properties to the energy-sharing fraction Q for PII was shown to be significant and much greater than that of EII. Thus large errors can result in real-world applications if PII is not treated carefully.

A simple energy-partition function was developed to capture qualitatively the underlying physics of PII. At high impact energies, the scattered positron leaves the collision with almost all of the available energy, while at near-threshold impact energies the Wannier theory [61] suggests that both the scattered positron and ejected electron share approximately half of the available energy. In reality, there is a slight energy-sharing asymmetry in near-threshold positron ionization [65] and a more sophisticated energy-partitioning model will need to take this asymmetry into account. The model parameters were fit to the experimental results of Kover and Laricchia [28] for positrons in H_2 with good qualitative agreement.

Using the H_2 energy-partitioning function constructed herein, we investigated the temporal relaxation of a positron swarm from a high-energy source (600 eV) to thermalization at room temperature and compared the equal-energy-sharing model with the common approach of treating the PII as a standard excitation process. In the ionization-dominated region there can be more than an order of magnitude in difference in the mean energy profiles and hence the choice of energy-partition function has a significant effect on the number of ionization collisions and the energy distribution of the secondary electrons created, which is particularly important for radiation damage modeling [9]. Our modeling also suggests that the spatial relaxation will be sensitive to the energy partitioning, which is a topic to be further investigated.

ACKNOWLEDGMENTS

This work was supported under the Australian Research Council's Centre of Excellence Discovery programs. The authors would like to thank Professor I. Bray and M. Zammit for helpful communications and cross-section calculations in H_2. S.D. acknowledges support from MPNTRRS Projects No. OI171037 and No. III41011.

APPENDIX A: DERIVATION OF POSITRON-IMPACT IONIZATION OPERATOR

The case of EII has been treated by Ness [20] and we follow this work closely to derive the PII collision operator. For simplicity, we consider one ionization process with a neutral in the ground state, but the generalization is straightforward. To derive the collision operator we consider the scattering of positrons into and out of an element of phase space $d\mathbf{r}d\mathbf{v}$.

Let us consider a beam of positrons incident upon the background neutrals that are at rest. The flux of incident positrons $\mathbf{I}$ in $d\mathbf{r}d\mathbf{v}$ is

$$\mathbf{I} = \mathbf{v} f(\mathbf{r},\mathbf{v},t)d\mathbf{v}.$$

If $\sigma^{\text{ion}}(v)$ is the total ionization cross section for an incoming positron of speed v, then the number of ionization collisions in $d\mathbf{r}d\mathbf{v}$ per unit time per neutral is

$$I\sigma^{\text{ion}}(v) = vf(\mathbf{r},\mathbf{v},t)\sigma^{\text{ion}}(v)d\mathbf{v}$$

and hence the total rate of positrons scattered out of the element $d\mathbf{r}d\mathbf{v}$ for n_0 neutral particles due to ionization is

$$J^{\text{ion}}_{\text{out}}(f)d\mathbf{r}d\mathbf{v} = n_0 v\sigma^{\text{ion}}(v)f(\mathbf{r},\mathbf{v},t)d\mathbf{r}d\mathbf{v}. \tag{A1}$$

In EII, either the primary or ejected electrons (which are indistinguishable) from an ionization event somewhere else in phase space may be scattered into the element $d\mathbf{r}d\mathbf{v}$. Since one can distinguish between electrons and positrons, the PII equivalent is simpler. Let us consider a different element of phase space with the same configuration space location but different velocity space location, i.e., $d\mathbf{r}d\mathbf{v}'$. Similar to (A1), the total number of PII in $d\mathbf{r}d\mathbf{v}'$ per unit time is

$$n_0 v'\sigma^{\text{ion}}(v')f(\mathbf{r},\mathbf{v}',t)d\mathbf{r}d\mathbf{v}'. \tag{A2}$$

The momentum postionization is shared between the scattered positron and the ejected electron. We define a quantity $B(\mathbf{v},\mathbf{v}')$ such that $B(\mathbf{v},\mathbf{v}')d\mathbf{v}$ is the probability of the positron having a velocity between $\mathbf{v}$ and $\mathbf{v}+d\mathbf{v}$ after ionization, given that the incident positron has velocity $\mathbf{v}'$. Assuming the neutral particle remains a bystander at rest during the process (to zeroth order in the mass ratio m/m_0), then by conservation of momentum

$$\mathbf{v}' = \mathbf{v} + \bar{\mathbf{v}},$$

where $\bar{\mathbf{v}}$ is the velocity of the ejected electron. It follows from Eq. (A2) and the definition of $B(\mathbf{v},\mathbf{v}')$ that the number of positrons that enter $d\mathbf{r}d\mathbf{v}$ per unit time due to an ionization event in $d\mathbf{r}d\mathbf{v}'$ is

$$n_0 v'\sigma^{\text{ion}}(v')f(\mathbf{r},\mathbf{v}',t)B(\mathbf{v},\mathbf{v}')d\mathbf{v}d\mathbf{r}d\mathbf{v}'.$$

Integrating over all possible incident velocities thus yields the total rate of positrons scattered into $d\mathbf{r}d\mathbf{v}$ due to PII, i.e.,

$$J^{\text{ion}}_{\text{into}}(f)d\mathbf{r}d\mathbf{v} = n_0 d\mathbf{r}d\mathbf{v}\int v'\sigma^{\text{ion}}(v')f(\mathbf{r},\mathbf{v}',t)B(\mathbf{v},\mathbf{v}')d\mathbf{v}'.$$

The total PII collision operator is then the difference in the rates of positrons scattered into and out of the element $d\mathbf{r}d\mathbf{v}$, i.e., $J^{\text{ion}} = J^{\text{ion}}_{\text{out}} - J^{\text{ion}}_{\text{into}}$,

$$J^{\text{ion}}(f) = n_0 v\sigma^{\text{ion}}(v)f(\mathbf{r},\mathbf{v},t) - n_0\int v'\sigma^{\text{ion}}(v')B(\mathbf{v},\mathbf{v}')f(\mathbf{r},\mathbf{v}',t)d\mathbf{v}'. \tag{A3}$$

If we assume central forces, then the scattering cross section and partition function are dependent only on the magnitudes of the pre- and postcollision velocities and the angle between them, i.e., v, v', and $\hat{\mathbf{v}}\cdot\hat{\mathbf{v}}'$. We may then further define a differential scattering cross section for ionization $\sigma^{\text{ion}}(v,v';\hat{\mathbf{v}}\cdot\hat{\mathbf{v}}')$ such that $\sigma^{\text{ion}}(v,v';\hat{\mathbf{v}}\cdot\hat{\mathbf{v}}')d\mathbf{v}$ is the number of positrons scattered into the range $d\mathbf{v}$ about $\mathbf{v}$ due to incident electrons of velocity $\mathbf{v}'$ divided by incident flux,

$$\sigma^{\text{ion}}(v,v';\hat{\mathbf{v}}\cdot\hat{\mathbf{v}}')d\mathbf{v} = \sigma^{\text{ion}}(v')B(v,v';\hat{\mathbf{v}}\cdot\hat{\mathbf{v}}')d\mathbf{v}. \tag{A4}$$

The partition function satisfies a normalization condition so that

$$\sigma^{\text{ion}}(v') = \int \sigma^{\text{ion}}(v,v';\hat{\mathbf{v}}\cdot\hat{\mathbf{v}}')d\mathbf{v}.$$

Substituting Eq. (A4) into Eq. (A3) gives the PII collision operator

$$J^{\text{ion}}(f) = n_0 v\sigma^{\text{ion}}(v)f(\mathbf{v}) - n_0\int v'\sigma^{\text{ion}}(v,v';\hat{\mathbf{v}}\cdot\hat{\mathbf{v}}')f(\mathbf{v}')d\mathbf{v}'.$$

This operator is particle-number conserving, i.e.,

$$\begin{aligned}\int J^{\text{ion}}(f)d\mathbf{v} &= \int n_0 v\sigma^{\text{ion}}(v)f(\mathbf{v})d\mathbf{v} - n_0\iint v'\sigma^{\text{ion}}(v,v';\hat{\mathbf{v}}\cdot\hat{\mathbf{v}}')f(\mathbf{v}')d\mathbf{v}'d\mathbf{v}\\ &= n_0\int v\sigma^{\text{ion}}(v)f(\mathbf{v})d\mathbf{v} - n_0\int v'f(\mathbf{v}')d\mathbf{v}'\int \sigma^{\text{ion}}(v,v';\hat{\mathbf{v}}\cdot\hat{\mathbf{v}}')d\mathbf{v}\\ &= n_0\int v\sigma^{\text{ion}}(v)f(\mathbf{v})d\mathbf{v} - n_0\int v'\sigma^{\text{ion}}(v')f(\mathbf{v}')d\mathbf{v}'\\ &= 0,\end{aligned}$$

as required.

1. Legendre decomposition

For central scattering forces the partition function can be decomposed in terms of Legendre polynomials, i.e.,

$$B_l(v,v') = 2\pi\int_{-1}^{1} B(\mathbf{v},\mathbf{v}')P_l(\mu)d\mu,$$

where $\mu = \hat{\mathbf{v}}\cdot\hat{\mathbf{v}}'$. For isotropic scattering, $B_l(v,v') = 0$ for $l \geqslant 1$. Multiplying Eq. (A3) by $P_l(\cos\chi)$ and integrating over all angles leads to

$$J^{\text{ion}}_l(f_l) = n_0 v\sigma^{\text{ion}}(v)f_l(v) - \begin{cases} n_0\int_0^\infty v'\sigma^{\text{ion}}(v')B_0(v,v')f_0(v')v'^2dv', & l=0\\ 0, & l\geqslant 1.\end{cases} \tag{A5}$$

We now seek to represent Eq. (A5) in terms of energy rather than speed, i.e., $U = \frac{1}{2}mv^2$. The probability of a positron having a speed in the range $v + dv$ after ionization for an incident positron of speed v' is

$$v^2dv\int B(v,v';\hat{\mathbf{v}}\cdot\hat{\mathbf{v}}')d\hat{\mathbf{v}} = B(v,v')v^2dv \equiv P(U,U')dU, \tag{A6}$$

TABLE IV. Comparison of average ionization rate α^{ion}/n_0, mean energies ε, flux drift velocities W_{flux}, and bulk drift velocities W_{bulk} for EII for model (10) for different reduced fields E/n_0 and energy-sharing fractions Q. The first column lists the current kinetic theory calculations, the second column lists the results of our Monte Carlo simulations, and the third includes the kinetic theory calculations of Ness and Robson [41]. The values enclosed in square brackets have been performed using a Burnett function expansion similar to that of Ness and Robson. A Q entry of AFE corresponds to all fractions equiprobable. Note that there was an error in the AFE case in the original Ness and Robson work [41].

E/n_0		α^{ion}/n_0 (10^{-15} m^3 s^{-1})			ε (eV)			W_{flux} (10^5 ms^{-1})		W_{bulk} (10^5 ms^{-1})		
(Td)	Q	Current	MC	[41]	Current	MC	[41]	Current	[41]	Current	MC	[41]
300	0		1.620	1.61		6.739	6.73		2.780		3.236	3.23
	1/4	1.598	1.611	1.60	6.737	6.741	6.73	2.752	2.754	3.200	3.204	3.20
	1/3	1.595	1.596	1.60	6.739	6.741	6.73	2.748	2.749	3.194	3.196	3.20
	1/2	1.591	1.589	1.59	6.742	6.744	6.74	2.744	2.745	3.189	3.192	3.19
	AFE	1.600	1.606	1.51	6.733	6.746	6.75	2.756	2.755	3.198	3.206	3.19
				[1.60]			[6.73]					[3.21]
500	0		4.643	4.68		9.009	8.99		3.920		4.752	4.74
	1/4	4.504	4.515	4.51	9.007	9.007	9.01	3.835	3.839	4.632	4.644	4.63
	1/3	4.482	4.492	4.49	9.013	9.023	9.01	3.823	3.822	4.617	4.617	4.62
	1/2	4.464	4.452	4.47	9.017	9.028	9.02	3.814	3.816	4.604	4.606	4.61
	AFE	4.511	4.525	4.37	9.000	9.007	9.04	3.846	3.843	4.635	4.647	4.62
				[4.52]			[9.00]					[4.64]
800	0		9.736	9.62		13.17	13.21		5.112		6.284	6.25
	1/4	9.413	9.422	9.41	13.01	13.02	13.01	4.953	4.957	6.108	6.118	6.11
	1/3	9.357	9.372	9.37	12.99	12.99	12.99	4.933	4.936	6.090	6.092	6.09
	1/2	9.320	9.339	9.33	12.97	12.98	12.97	4.919	4.922	6.079	6.095	6.08
	AFE	9.461	9.445	9.20	13.03	13.02	13.09	4.968	4.976	6.137	6.137	6.12
				[9.46]			[13.02]					[6.13]

where U and U' are the post- and precollision positron energies respectively, and now the right-hand-side term of Eq. (A6) represents the probability of a positron having an energy in the range $U + dU$ after ionization for an incident positron of U'. The energy-partitioning function $P(U,U')$ has the following properties:

$$P(U,U') = 0, \quad U' < U + U_I$$
$$\int_0^{U'-U_I} P(U,U')dU = 1, \quad U' \geqslant U + U_I.$$

Finally, we can represent Eq. (A5) in terms of energy and the energy-partition function $P(U,U')$,

$$J_l^{\text{ion}}(f_l) = n_0\sqrt{\frac{2U}{m}}\sigma^{\text{ion}}(U)f_l(U) - \begin{cases} n_0\sqrt{\frac{2}{mU}}\int_0^\infty U'\sigma^{\text{ion}}(U')P(U,U')f_0(U')dU', & l = 0 \\ 0, & l \geqslant 1. \end{cases} \tag{A7}$$

2. Modified Frost-Phelps operator

If the scattered positron leaves the collision with an exact fraction Q of the available energy $U' - U_I$, where U_I is the threshold energy, then the energy-partition function has the form

$$P(U,U') = \delta(U - Q(U' - U_I)) = \frac{1}{Q}\delta\left(U' - \left(\frac{U}{Q} + U_I\right)\right)$$

and the integral in Eq. (A7) reduces to

$$J_l^{\text{ion}}(f_l) = \nu^{\text{ion}}(U)f_l(U) - \begin{cases} \frac{1}{Q}\frac{(U/Q+U_I)^{1/2}}{U^{1/2}}\nu^{\text{ion}}\left(\frac{U}{Q}+U_I\right)f_0\left(\frac{U}{Q}+U_I\right), & l = 0 \\ 0, & l \geqslant 1, \end{cases} \tag{A8}$$

where $\nu^{\text{ion}}(U) = n_0\sqrt{2U/m}\sigma^{\text{ion}}(U)$ is the ionization collision frequency. Equation (A8) can be considered a modified Frost-Phelps operator. A similar result for EII was given in [69]. In the case where the positron gets all of the available energy, i.e., $Q = 1$, Eq. (A8) reduces to the standard Frost-Phelps operator (5), as required. Clearly, Eq. (A8) breaks down when $Q = 0$.

APPENDIX B: ELECTRON-IMPACT IONIZATION BENCHMARKS

Transport coefficients for EII are given in Table IV, in which they are compared to the results of Ness and Robson [41]. Due to the indistinguishability of postcollision particles, the results for Q and $1 - Q$ with respect to EII are identical and so we consider only $Q < 0.5$. The modified Frost-Phelps form of the collision operator (A8) breaks down when $Q = 0$, hence there is no value given in Table IV corresponding to $Q = 0$ and 1 (if one of the electrons gets the fraction $Q = 1$ of the available energy, then the other receives $Q = 0$ and the same problem is encountered). The EII calculations using our kinetic theory model agree closely with both our Monte Carlo simulations and the kinetic theory approach in [41]. There are generally differences of less than 0.6% and 0.3% in the ionization rate and mean energy, respectively, between the present kinetic theory results and both the Monte Carlo simulation and [20] over the whole range of reduced fields and energy-sharing fractions, except for the AFE case. An error is present in the AFE calculations of [20]. Values for the AFE case have been recalculated using a Burnett function [70] expansion similar to that of Ness and Robson (which are included in Table IV enclosed within square brackets), which agree closely with our calculations. In Ref. [20], the bulk drift velocities are given, which must not be confused with the flux drift velocity [71–73]. The two types of transport coefficients can be significantly different when there are nonconservative effects. Following [73] we have solved the first level of spatially inhomogeneous equations, which come from a density gradient expansion [70], in addition to Eq. (3) to determine the bulk drift velocity. Both the flux and bulk drift velocities generally agree to within 0.3% between the three calculation methods over the range of fields and energy-sharing fractions considered.

[1] T. J. Murphy and C. M. Surko, Phys. Rev. A **46**, 5696 (1992).
[2] R. Greaves, M. Tinkle, and C. Surko, Phys. Plasmas **1**, 1439 (1994).
[3] P. Coleman, Nucl. Instrum. Methods Phys. Res. Sect. B **192**, 83 (2002).
[4] Z. Petrovic, A. Bankovic, S. Dujko, S. Marjanovic, G. Malovic, J. Sullivan, and S. Buckman, in *Proceedings of the Eighth International Conference on Atomic and Molecular Data and Their Applications*, edited by J. D. Gillaspy, W. L. Wiese, and Y. A. Podpaly, AIP Conf. Proc. No. 1545 (AIP, New York, 2013), p. 115.
[5] A. Panov, J. Phys.: Conf. Ser. **409**, 012004 (2013).
[6] J. Czernin and M. Phelps, Annu. Rev. Med. **53**, 89 (2002).
[7] L. Sanche, Phys. Scr. **68**, C108 (2003).
[8] L. Sanche, Eur. Phys. J. D **35**, 367 (2005).
[9] L. Sanche, in *Radiation Induced Molecular Phenomena in Nucleic Acids: A Comprehensive Theoretical and Experimental Analysis*, edited by M. Shukla and J. Leszczynski (Springer, Rotterdam, 2008).
[10] L. Sanche, *Radical and Radical Ion Reactivity in Nucleic Acid Chemistry* (Wiley, Hoboken, 2009).
[11] I. Abril, R. Garcia-Molina, C. Denton, I. Kyriakou, and D. Emfietzoglou, Radiat. Res. **175**, 247 (2011).
[12] V. Cobut, Y. Frongillo, J. P. Patau, T. Goulet, M.-J. Fraser, and J.-P. Jay-Gerin, Radiat. Phys. Chem. **51**, 229 (1998).
[13] M. Charlton and J. Humberston, *Positron Physics* (Cambridge University Press, Cambridge, 2001).
[14] *Proceedings of the Third International Workshop on Positron (Electron)-Gas Scattering*, edited by W. E. Kauppila, T. S. Stein, and J. Wadehra (World Scientific, Singapore, 1986).
[15] D. Loffhagen and R. Winkler, J. Phys. D **29**, 618 (1996).
[16] K. F. Ness and A. M. Nolan, Aust. J. Phys. **53**, 437 (2000).
[17] R. Winkler, D. Loffhagen, and F. Sigeneger, Appl. Surf. Sci. **192**, 50 (2002).
[18] G. Grubert and D. Loffhagen, J. Phys. D **47**, 025204 (2014).
[19] S. Dujko, M. Raspopovic, R. White, T. Makabe, and Z. Petrovic, Eur. Phys. J. D **68**, 166 (2014).
[20] K. Ness, Ph.D. thesis, James Cook University, Australia, 1985.
[21] M. Suvakov, Z. Petrovic, J. Marler, S. Buckman, R. Robson, and G. Malovic, New J. Phys. **10**, 053034 (2008).
[22] J. Marler, Z. Petrovic, A. Bankovic, S. Dujko, M. Suvakov, G. Malovic, and S. Buckman, Phys. Plasmas **16**, 057101 (2009).
[23] R. D. White and R. E. Robson, Phys. Rev. Lett. **102**, 230602 (2009).
[24] R. D. White and R. E. Robson, Phys. Rev. E **84**, 031125 (2011).
[25] A. Bankovic, S. Dujko, R. White, S. Buckman, S. Marjanovic, G. Malovic, G. Garcia, and Z. Petrovic, New J. Phys. **14**, 035003 (2012).
[26] A. Bankovic, S. Dujko, R. White, S. Buckman, and Z. Petrovic, Nucl. Instrum. Methods Phys. Res. Sect. B **279**, 92 (2012).
[27] Z. Petrovic, S. Marjanovic, S. Dujko, A. Bankovic, G. Malovic, S. Buckman, G. Garcia, R. White, and M. Brunger, Appl. Radiat. Isotopes **83**, 148 (2014).
[28] A. Kover and G. Laricchia, Phys. Rev. Lett. **80**, 5309 (1998).
[29] C. Cercignani, *The Boltzmann Equation and Its Applications* (Springer, New York, 1998).
[30] R. E. Robson, R. Winkler, and F. Sigeneger, Phys. Rev. E **65**, 056410 (2002).
[31] M. Abramowitz and I. A. Stegun, *Handbook of Mathematical Functions* (Dover, New York, 1972).
[32] L. Huxley and R. Crompton, *The Diffusion and Drift of Electrons in Gases* (Wiley, New York, 1974).
[33] R. D. White, R. E. Robson, B. Schmidt, and M. A. Morrison, J. Phys. D **36**, 3125 (2002).
[34] G. J. Boyle, R. P. McEachran, D. G. Cocks, and R. D. White, J. Chem. Phys. **142**, 154507 (2015).
[35] R. E. Robson, *Introductory Transport Theory for Charged Particles in Gases* (World Scientific, Singapore, 2006).
[36] H. Goldstein, C. P. Poole, and J. F. Safko, *Classical Mechanics*, 3rd ed. (Addison-Wesley, Boston, 2001).
[37] C. Wang-Chang, G. Uhlenbeck, and J. D. Boer, in *Studies in Statistical Mechanics* (Wiley, New York, 1964), Vol. II, p. 241.
[38] B. Davydov, Phys. Z. Sowjetunion **8**, 59 (1935).
[39] L. Frost and A. Phelps, Phys. Rev. **127**, 1621 (1962).
[40] T. Holstein, Phys. Rev. **70**, 367 (1946).
[41] K. F. Ness and R. E. Robson, Phys. Rev. A **34**, 2185 (1986).
[42] L. F. Shampine, Numer. Methods Partial. Differ. Eq. **10**, 739 (2005).
[43] M. N. O. Sadiku and C. N. Obiozor, Int. J. Electr. Eng. Ed. **37**, 282 (2000).
[44] M. B. Carver and H. W. Hinds, Simulation **31**, 59 (1978).
[45] J. C. Butcher, *Numerical Methods for Ordinary Differential Equations* (Wiley, Hoboken, 2003).

[46] R. Burden and D. Faires, *Numerical Analysis*, 5th ed. (Weber and Schmidt, Boston, 1993).
[47] R. LeVeque, *Finite Difference Methods for Ordinary and Partial Differential Equations* (SIAM, Philadelphia, 2007).
[48] R. Winkler, G. L. Braglia, A. Hess, and J. Wilhelm, Beitr. Plasmaphys. **24**, 657 (1984).
[49] H. Leyh, D. Loffhagen, and R. Winkler, Comput. Phys. Commun. **113**, 33 (1998).
[50] R. Campeanu and J. Humberson, J. Phys. B **10**, 239 (1977).
[51] R. D. White, M. J. Brennan, and K. F. Ness, J. Phys. D **30**, 810 (1997).
[52] Z. M. Raspopovic, S. Sakadzic, S. A. Bzenic, and Z. L. Petrovic, IEEE Trans. Plasma Sci. **27**, 1241 (1999).
[53] W. J. Tattersall, D. G. Cocks, G. J. Boyle, S. J. Buckman, and R. D. White, Phys. Rev. E **91**, 043304 (2015).
[54] L. Devroye, *Non-Uniform Random Variate Generation* (Springer, New York, 1986).
[55] T. E. Booth, Los Alamos National Laboratory Report No. LA-10363-MS, 1985.
[56] J. Lucas and H. Saelee, J. Phys. D **8**, 640 (1975).
[57] T. Taniguchi, H. Tagashira, and Y. Sakai, J. Phys. D **10**, 2301 (1977).
[58] K. Ness and T. Makabe, Phys. Rev. E **62**, 4083 (2000).
[59] D. Trunec, Z. Bonaventura, and D. Necas, J. Phys. D **39**, 2544 (2006).
[60] M. Brauner and J. Briggs, J. Phys. B **19**, L325 (1986).
[61] G. Wannier, Phys. Rev. **90**, 817 (1953).
[62] H. Klar, J. Phys. B **14**, 4165 (1981).
[63] P. Ashley, J. Moxom, and G. Laricchia, Phys. Rev. Lett. **77**, 1250 (1996).
[64] W. Ihra, J. H. Macek, F. Mota-Furtado, and P. F. O'Mahony, Phys. Rev. Lett. **78**, 4027 (1997).
[65] C. Arcidiacono, A. Kover, and G. Laricchia, Phys. Rev. Lett. **95**, 223202 (2005).
[66] M. Brauner, J. Briggs, and H. Klar, J. Phys. B **22**, 2265 (1989).
[67] M. Zammit (private communication).
[68] M. C. Zammit, D. V. Fursa, and I. Bray, Phys. Rev. A **87**, 020701(R) (2013).
[69] F. Sigeneger and R. Winkler, Plasma Chem. Plasma Process. **17**, 281 (1997).
[70] K. Kumar, H. Skullerud, and R. Robson, Aust. J. Phys. **33**, 343 (1980).
[71] Y. Sakai, H. Tagashira, and S. Sakamoto, J. Phys. D **10**, 1035 (1977).
[72] H. Tagashira, Y. Sakai, and S. Sakamoto, J. Phys. D **10**, 1051 (1977).
[73] R. E. Robson and K. F. Ness, Phys. Rev. A **33**, 2068 (1986).